Particle simulation of plasma turbulence and neoclassical E_r at tokamak plasma edge

T.P. Kiviniemi[1], J.A. Heikkinen[2], S. Janhunen[1], T. Kurki-Suonio[1], S.K. Sipilä[1]

[1]Association Euratom-Tekes, Helsinki University of Technology, Finland
[2]Association Euratom-Tekes, VTT Processes, Finland

email: Timo.Kiviniemi@hut.fi

Abstract. Particle simulations of turbulence, L–H transition and neoclassical electric field for various tokamaks both near the edge and inside the plasma are presented. Five dimensional Monte Carlo guiding centre orbit following code ASCOT, which simulates neoclassical physics, and its gyrokinetic upgrade ELMFIRE, which takes into account also electrostatic turbulence, are used.

1. Introduction

Particle simulation is a powerful tool in tokamak plasma research especially near the edge where mechanisms like ion orbit loss, finite orbit effects with steep background gradients, and recycling call for a kinetic solution rather than the conventional fluid approach. This is the case also for the simulation of radial electric field, E_r. In Ref. [1], for the first time, E_r was obtained from simulations with a fully kinetic five-dimensional (three dimensions in configuration space and two velocity dimensions) neoclassical Monte Carlo guiding-center orbit-following code ASCOT [2] for the tokamak plasma edge in a realistic ASDEX Upgrade and JET divertor geometry. It was shown that high enough shear for turbulence suppression can be driven without taking into account anomalous processes in E_r shear formation. A good agreement between these ASCOT results and E_r simulated with the two-dimensional fluid code B2SOLPS5.0 was found in Ref. [3] and in Ref. [4], a fairly similar code gave similar results.

In plasma turbulence research, for the core plasma, most gyrokinetic simulations are currently performed exploiting nonlinear δf techniques. It is believed that the δf method may become too cumbersome for the collisional edge plasma with steep gradients, fast transients, strong recycling and orbit losses. For this reason, an efficient full-f gyrokinetic particle model has been developed for the investigation of self-consistent particle orbits and potential fluctuations at the edge of a tokamak, together with basic neoclassical phenomena of such plasmas [5].

In Section 2, the numerical techniques are presented. Results of the simulation of neoclassical radial electric field in ASDEX Upgrade and JET using ASCOT are reviewed in Section 3. In Section 4, simulations carried out both with ASCOT and its gyrokinetic upgrade ELMFIRE, that takes into account also the turbulent effects, are presented for FT–2 tokamak. In Section 5, conclusions are presented.

2. Numerical methods

In ASCOT, each particle is followed along its guiding-center orbit determined by various drifts ($\mathbf{E} \times \mathbf{B}$, gradient, curvature, polarization and gyroviscosity drifts) and collisions. The particle following takes place in a realistic geometry including the region outside the separatrix. The magnetic background is assumed stationary. In order to properly treat the momentum equation and momentum generation, a binary collision model that conserves momentum and energy in pairwise collisions between the ions has been implemented but, alternatively, collisions with the fixed background can also be used. For a fixed electric field $\vec{E}$ and for a field obtained from the 1-D (radial) polarization equation, the adopted numerical model has been tested by calculating poloidal rotation relaxation rates for a homogeneous plasma, and by comparing the perpendicular conductivity and parallel viscosity evaluated by the code with analytical expressions. In studies of transport processes, ASCOT is limited to neoclassical physics caused by Coulomb collisions, which gives a lower bound to transport in tokamaks. It is suitable tool for investigating many phenomena where turbulence does not play a major role and a number of diagnostics has been developed for ASCOT over the years. For more detailed description of the ASCOT code see Ref. [2].

In gyrokinetic version of ASCOT, ELMFIRE, 3D electric perturbations are solved allowing investigation of the turbulent phenomena in addition to neoclassical effects. The full-f plasma quasi-neutrality is solved using an implicit method where the ion density change by polarization drift is evaluated directly from the ion orbit motion in terms of the unknown electrostatic potential at each time step. Since this discrete operator is sampled directly from the particle distribution, strong non-Maxwellian deviations in velocity distributions and large deviations in background distribution are allowed. The guiding-center equations, the implementation of binary collisions to conserve momentum and energy between the particles, the fixed magnetic configuration, and the quiescent particle initialization method are the same as in ASCOT, thus making it possible to simulate neoclassical physics (simultaneously with the turbulence) avoiding the limitations of the former methods. The electrons are treated either adiabatically, keeping a fixed electron distribution, or following their orbits in the drift-kinetic approximation. The code is able to simulate turbulent effects, such as ion temperature gradient modes and trapped electron modes, while consistently simulating the neoclassical electric field affecting these modes. A detailed description of numerical methods can be found in Ref. [5].

3. Neoclassical simulations in realistic tokamak geometries

There are very few simulations of the radial electric field at the edge in realistic tokamak geometry as a function of the local plasma parameters. In Ref. [1] fully kinetic ASCOT simulations were carried out. In these simulations, the plasma temperature, density, and toroidal magnetic field were varied over a wide parameter range of ASDEX Upgrade and JET data across the experimental L–H transition conditions. In Fig. 1, the $E \times B$ shearing rate $\omega_s \approx (1/B)|\mathrm{d}E_r/\mathrm{d}r|$ from this series of simulations is shown. Here, AUG and JET1 refer to experimental data at L–H transition conditions at ASDEX Upgrade and JET, respectively. For comparison, some data points using the scale

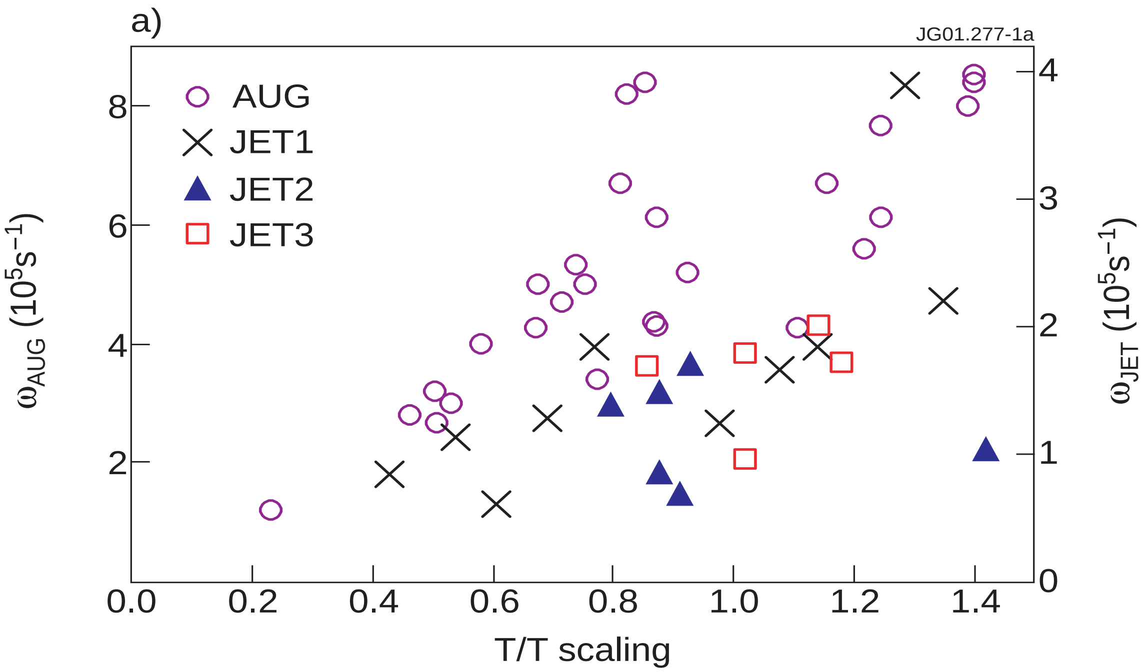

Figure 1: $E \times B$ shearing rate from a series of ASCOT simulations around the experimental L–H transition conditions. Temperature on the horizontal axis is normalized to the scaling of the experimental L–H transition temperature.

lengths of L–mode (JET2) and H–mode (JET3) profiles are also included, but again, the magnetic field, temperature and density are varied across the values at which experimental scaling predicts L–H transition. In Ref. [6], similar scans have been done with the two-dimensional B2SOLPS5.0 fluid code (for the description of the code, see Ref. [7]) for ASDEX Upgrade. The code solves the most complete system of transport equations, and the geometry is realistic including shape effects such as elongation and triangularity. Both ASCOT and B2SOLPS5.0 give similar scaling $\omega_s \approx |\alpha T_i/B|\, s^{-1}$ with the coefficient $\alpha = 5.4 \times 10^3$ from B2SOLPS5.0 or $\alpha = 4.6 \times 10^3$ from ASCOT for typical ASDEX Upgrade parameters. Here, T_i is expressed in eV, B in Tesla. However, in Ref. [1] the significance of ion orbit losses, not included in Ref. [6], is emphasized. On the other hand, Ref. [6] concludes that the anomalous viscosity and the consequent parallel velocity are of major importance in determining E_r while in Ref. [1] anomalous effects are neglected and the averaged parallel velocity is kept small. $\vec{E_r} \times \vec{B}$ shear values are high enough for turbulence suppression but, as discussed in Refs. [1, 6], we have not observed any bifurcation; instead the field changes smoothly as a function of temperature even in the banana limit. The results give further proof and confidence on the mostly neoclassical nature of the electric field at L–H transition. The turbulence theory is only called for to give a criterion for high enough shear for turbulence suppression and to explain some details of transition. Simulations do not explain the fast time scale of the transition, but a parameter dependence of the transition temperature consistent with experiment is found with both codes, and the fluid simulation is also able to explain the change in L–H transition power threshold when the direction of ∇B drift is changed.

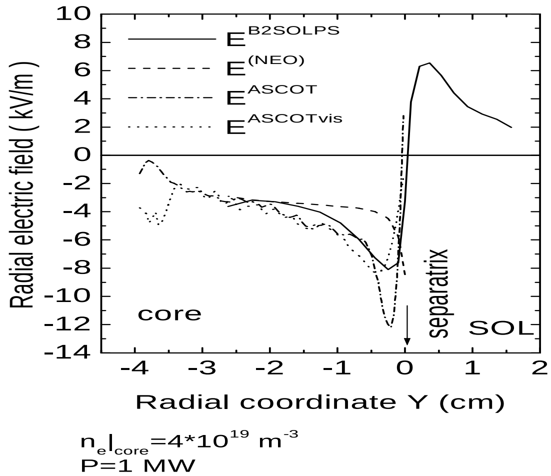

Figure 2: *E_r at the outer midplane from B2SOLPS5.0, ASCOT and from analytic theory for ASDEX Upgrade parameters. The analytic curve $E^{(NEO)}$ is calculated for $\langle V_\parallel \rangle$ from B2SOLPS5.0.*

As an example of this benchmarking, in Fig. 2 the radial electric fields at the outboard equator are plotted as a function of the radial distance from the separatrix on the outboard equator for a separatrix temperature $T_{i,sep} = 105$ eV (corresponding to input power $P = 1$ MW). The collisionality in the simulation regime varies between $3.8 < \nu_{*i} < 4.7$. The analytic result [8], determined at outboard equator and calculated for $\langle V_\parallel \rangle$ from B2SOLPS5.0, is shown together with the results of both codes. In the main part of the core region the agreement between ASCOT and B2SOLPS5.0 results is quite good. One difference is the dip at the separatrix, which is more pronounced in the ASCOT runs with the classical viscosity. This can be explained by orbit losses which are self-consistently included in ASCOT but not in B2SOLPS5.0. With radial current driven by anomalous viscosity the narrow electric field structure of ASCOT becomes smoother and the structure of the dip at the separatrix looks now similar for both codes.

4. Formation of ITB in FT-2

In the low current ($I = 22$ kA, $B_T = 2.2$ T) small ($R = 55$ cm, $a = 8$ cm) FT-2 tokamak, when the auxiliary heating provided by Lower Hybrid (LH) waves is combined with a global shifting of the plasma column and/or a current ramp-up, a transition into an improved confinement mode has been observed [9]. In some discharges the plasma profiles and the neutral particle analyzer (NPA) data suggest that the transport barrier associated with the improved confinement is created near the plasma periphery (H-mode with edge transport barrier, ETB), while other discharges indicate improved core confinement (ICC) and an internal transport barrier (ITB).

FT-2 has several features that make it a very attractive tokamak for studying the relevance of neoclassical effects in E_r generation: it has a large ripple (leading to direct losses and stochastic diffusion), very small poloidal field (leading to large orbit widths), and a heating method that creates high energy ions on wide orbits. In this work, the formation of an ITB in FT-2 in the presence of LH-waves is studied using ASCOT. However, turbulent effects such as Reynolds stress may also play a role. The effect of LH-waves is included using Monte Carlo operators [10] that give the change in the particle perpendicular energy $W_\perp$, the magnetic surface coordinate ρ, and the toroidal momentum p_ϕ. It is worth noting that the LH-interaction increases only the perpendicular energy and thus it moves ions across the trapped-passing boundary in the velocity space, thereby producing very wide drift orbits and increasing the direct orbit loss probability. Such things as rational surfaces, magnetic shear etc. can also have effect on the formation of ITB but these effects are omitted.

The ASCOT simulations were carried out for Ohmic, L-mode and ICC-mode conditions using 800.000 test particles that were followed for 0.5 ms. This time is sufficiently longer than both the ion-ion collision time and the bounce time. Radially the region of interest spans from $r = 2$ cm to $r = 8$ cm. Steady-state E_r was solved assuming parabolic plasma profiles: $n, T = n, T_0(1-\rho^2)^{\alpha_{n,T}} + n, T_{edge}$, where n_0, T_0, n_{edge} and T_{edge} are given in Table 1. The plasma current was $I_p = 22$ kA with a purely parabolic current density profile $j = j_0(1-\rho^2)$.

Table 1. Temperature and density profiles.

case	T_0 (eV)	T_{edge} (eV)	n_0 (m^{-3})	n_{edge} (m^{-3})	α_n	α_T
Ohmic	100	10	3e19	0.3e19	3	1
L–mode	200	20	4e19	0.3e19	1.5	1
ICC-mode	300	15	5e19	0.3e19	2.5	1.5

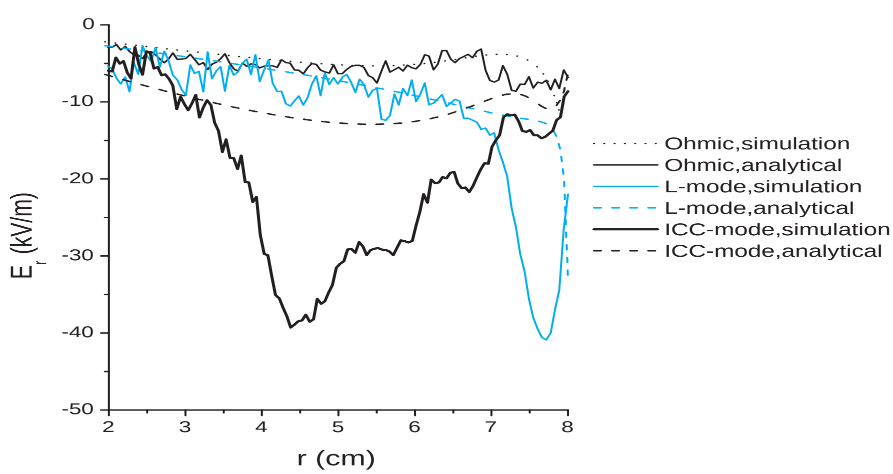

Figure 3: *Simulated E_r field profiles in a) Ohmic, b) L–mode, c) ICC-mode plasmas in FT-2 tokamak.*

Figure 3 shows the E_r profiles obtained for the different confinement mode phases. In the Ohmic phase the E_r profile agrees well with the standard neoclassical value [8] indicated by the dashed curve. In the L-mode phase the E_r profile is seen to deviate from

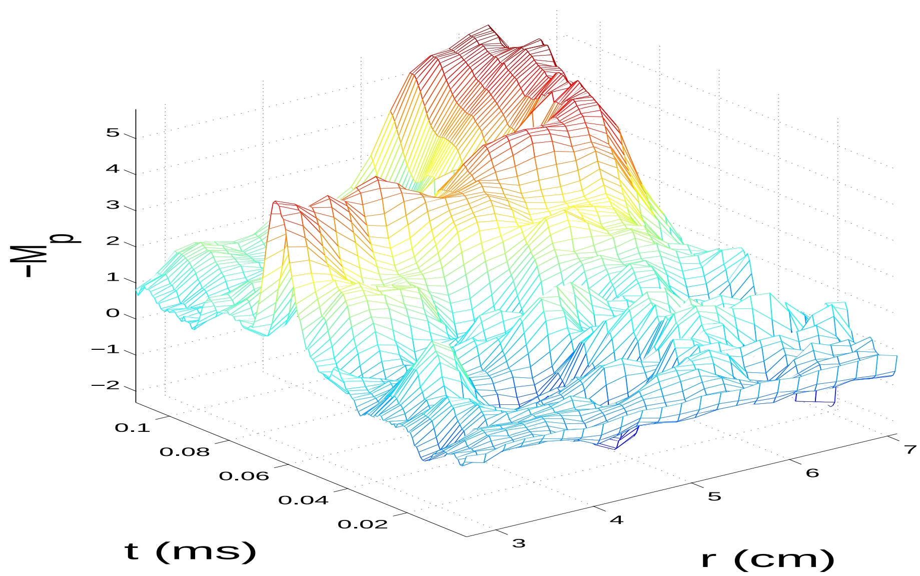

Figure 4: *Rapid growth in poloidal Mach number is observed when ITB develops.*

the corresponding neoclassical values at the edge. This is because the temperature is higher and so the orbit losses generate a non-ambipolar outward flux that induces the radial electric field in the plasma periphery, but only in a very narrow layer. Under certain conditions also an ITB-like structure is observed to form, i.e. during the simulation a deep electric field well is formed around the mid-radius. This field structure can be significantly stronger than what is formed in the edge region, and it is unlikely that direct losses to the wall or limiter are responsible for the generation of this field. Figure 3 also shows the E_r profile obtained for the ICC-mode displaying these features. A more detailed description of these simulations can be found in Ref. [11].

A similar simulation was repeated with the ELMFIRE code for a deuterium plasma. However, now the number of test particles is 10 million which is an order of magnitude more than needed in neoclassical simulations. At the outer edge, neutral particle ionization close to the limiter (with 1 cm decay length) provides the source of cold electron-ion pairs (at 15 eV) to replace the lost particles to the limiter. We have started the simulation either from the $T_e \sim 300$ eV, $T_i \sim 120$ eV plasma just after the onset of the 100 kW LH heating for ions (as in experiments) or from a well-heated plasma with $T_i \sim 250$ eV. The density and temperature profiles are taken to be close to the experimentally measured ones at the beginning of the simulation. For the case, where the initial conditions are close to that of the observed ITB generation (high ion temperature), the poloidal Mach number $M_p = E_r/B_p v_t$ (magnetic surface averaged) evolves as in Fig. 4. Interestingly, after some 60 μs the radial electric field increases significantly in the middle of the plasma, leading to a relatively strong shear in the $E_r \times B$ velocity at the radius $r \sim 6$ cm. This leads to a simultaneously appearing knee-point in the ion temperature profile at $r \sim 6$ cm and a rapid collapse of the heat and particle diffusion coefficients inside this radius. Thus, struture consistent with ITB formation was found in the simulation.

The diagnostics for turbulence show simultaneous suppression of broadband modes and related $\vec{E} \times \vec{B}$ convective cells together with the reduction of the size of the cells. The appearance of the transport barrier is found for both deuterium and hydrogen plasmas (only hydrogen was used in experiments) roughly at the same axis ion temperature threshold of 250 eV. Also, when the plasma is allowed to be heated gradually (in $100 - 200$ μs) from $T_i \sim 100$ eV, the transition occurs when the ion temperature reaches the above threshold. Inside the position of the ITB, both the ion particle diffusion (as shown in Fig. 5a) and the ion heat diffusion coefficient drop to values < 1 m^2/s after the transition, i.e., close to values obtained in ASTRA interpretative modeling of the FT-2 discharge.

The strong growth of M_p is also obtained when surface-averaged samples of ion and electron densities are used in the gyrokinetic equation, i.e., when the turbulence is suppressed. This implies that the effect seen in Fig. 4 arises from neoclassical effects, consistent with the results obtained in ASCOT simulations. In agreement with the ASCOT simulations, no strong potential difference is found at high plasma currents $I > 35$ kA, and no transport barrier is observed in line with experimental observations in FT-2. However, one should note that the code records a considerable Reynolds stress at the position of ITB at the time of its formation as shown in Fig. 5b.

5. Conclusions

In neoclassical ASCOT simulations for ASDEX Upgrade and JET, it was shown that high enough shear for turbulence suppression can be driven without taking into account anomalous processes in E_r shear formation. This has been further confirmed in simulations for the small-current tokamak FT–2. Simulations including both turbulence and neoclassical effects were also carried out with qualitatively similar results as in pure neoclassical simulation. Evidence of ITB generation was observed in transport coefficients in close agreement with experimental observations. Thus, it will be interesting to continue the work by repeating the simulations with turbulence for ASDEX Upgrade, which is a major numerical challenge.

Acknowledgements: The computing facilities of CSC – Scientific Computing Ltd were used in this work.

References

[1] HEIKKINEN, J. et al., Phys. Rev. Lett. **84**, (2000) 487; KIVINIEMI, T. et al., Plasma Phys. Contr. Fusion. **43** (2001) 1103.

[2] HEIKKINEN J. et al., J. Comput. Phys. **173** (2001) 527.

[3] KIVINIEMI, T. et al., Phys. Plasmas **10**, 2604 (2003).

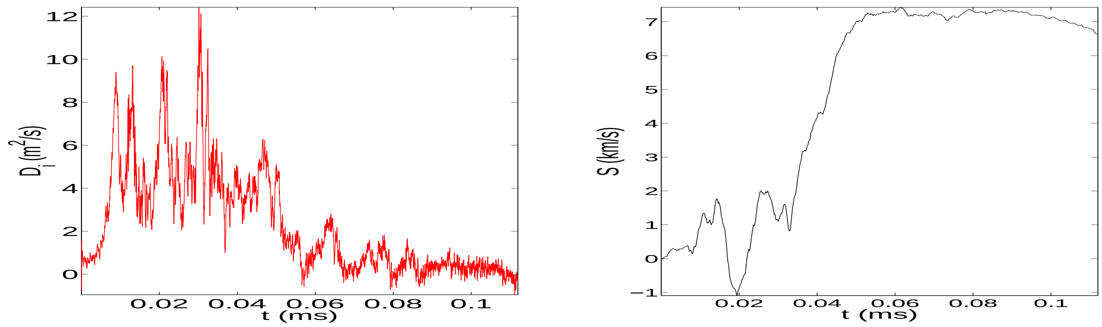

Figure 5: *a) Particle diffusion coefficient D_i and b) Reynolds stress at $r = 5$ cm.*

[4] CHANG C. et al., Phys. Plasmas **9**, 3884 (2002).

[5] HEIKKINEN J. et al., to be submitted to J. Comput. Phys.

[6] ROZHANSKY V. et al., Nucl. Fusion **42** (2002) 1110.

[7] ROZHANSKY V. et al., Nucl. Fus.**41** (2001) 387; ROZHANSKY V. et al., Contrib. Plasma Phys. **40** (2000) 423; SCHNEIDER R. et al., Contrib. Plasma Phys. **40** (2000) 328.

[8] HINTON F. et al., Rev. Mod. Phys. **48**, 239 (1976).

[9] LASHKUL S. et al., Proc. of the 27^{th} EPS Conf. on Contr. Fusion and Plasma Phys. (2000) p. 508.

[10] HEIKKINEN J. et al., Phys. Plasmas **2**, 3724 (1995).

[11] KURKI-SUONIO T. et al., Plasma Phys. Controll. Fusion 44 (2002) 301.